Contents lists available at SciOpen

Food Science and Human Wellness

journal homepage: https://www.sciopen.com/journal/2097-0765

China Food Publishing Co.

Preparations of *Mytilus edulis* protein hydrolysate-iron complexes and their ameliorative effects on mice with iron deficiency anemia

Guang Li[a,b], Xuening Yu[b], Shuling Zhou[b], Xiaoyang Liu[b,*], Fawen Yin[b], Deyang Li[b], Baocai Xu[a], Dayong Zhou[b]

[a] School of Food and Biological Engineering, Hefei University of Technology, Hefei 230601, China
[b] SKL of Marine Food Processing & Safety Control, National Engineering Research Center of Seafood, Collaborative Innovation Center of Seafood Deep Processing, Liaoning Province Key Laboratory for Marine Food Science and Technology, School of Food Science and Technology, Dalian Polytechnic University, Dalian 116034, China

ARTICLE INFO

Article history:
Received 26 May 2024
Received in revised form 18 July 2024
Accepted 24 October 2024

Keywords:
Iron deficiency anemia
Iron-chelating hydrolysate
Ameliorative
Oxidation stress
Colonic inflammation

ABSTRACT

Iron is a fundamental trace element essential for the immune system, and current research on iron (Fe) supplements is increasingly focusing on food-derived peptides capable of binding iron ions. The objectives of this study were to characterize the iron-chelating peptide (*Mytilus edulis* protein hydrolysate, MEPH) derived from *M. edulis* and to investigate the effects of MEPH-Fe complexes on mice with iron deficiency-induced iron deficiency anemia (IDA). MEPH and iron (II) sulfate heptahydrate successfully formed MEPH-Fe complexes under conditions of 4.5 mg/mL of concentration, 45 ℃, 60 min of incubation, and utilizing both carboxyl and amino binding sites. Compared to MEPH alone, the MEPH-Fe complexes exhibited fluorescence quenching, ultraviolet shifts, reduced X-ray diffraction (XRD) peak intensities, stabilization during *in vitro* digestion, microstructural changes, increased particle size, and decreased absolute values of Zeta potential. In the IDA mouse model, the MEPH-Fe complexes were able to restore body weight, hematological indices, organ coefficients, iron content in organs, and antioxidant capacity to normal levels. Additionally, they demonstrated beneficial effects on IDA-induced colonic inflammation by normalizing tumor necrosis factor-alpha (TNF-α) and interleukin-10 (IL-10) levels. The results indicated that MEPH-Fe complexes had more positive effects on IDA mice compared to ferrous sulfate. In conclusion, this study provides valuable insights into the potential of MEPH-Fe complexes as iron supplements.

1. Introduction

Iron is an essential micronutrient for the human body and has significant responsibilities in the metabolic processes of the body, such as the storage and transportation of oxygen[1]. However, iron deficiency is one of the most common nutritional deficiencies in the world[2], resulting in the phenomenon that one third of the world's population suffers from iron deficiency anemia (IDA) especially in proportion of the elderly, infants and pregnancy[3]. IDA could cause weight loss in children, respiratory and intestinal infections, and reduce fitness in adults[4]. Therefore, the intake of additional iron supplements becomes especially important.

The main common iron supplements on the market are iron salts and iron organic acids. However, these iron supplements are not only underutilized in the human gastrointestinal (GI) tract but also induce inflammation in the intestinal system[1]. As a result,

* Corresponding author at: School of Food Science and Technology, Dalian Polytechnic University, Dalian 116034, China
E-mail: liuxiaoyang0213@126.com (X.Y. Liu).
Peer review under responsibility of Beijing Academy of Food Sciences.

SciOpen Publishing services by Tsinghua University Press

http://doi.org/10.26599/FSHW.2024.9250439

research on iron supplements has gradually shifted to food-derived macromolecules that could be able to bind with the iron ion and is classified as the peptide-iron complex, which is considered to possess the iron absorption-promotive effects in the human GI tract. Food-derived peptide-iron complexes are considered to be effective substances for improving the symptoms of iron deficiency due to their superior bioavailability, absorption and stability[5]. Recent studies have reported the restorative effects of peptides derived from different substances chelated with iron ions to form biologically active peptide-iron complexes against IDA in established IDA animal models. In animal models, IDA has been shown to affect diet and growth, hematologic and visceral markers, the immune regulatory system, increase inflammation levels, compromise the intestinal mucosal barrier, and cause imbalances in the intestinal flora of mice[6]. Iron salt supplements (for example, ferrous sulfate), despite their positive effects on certain hematological indicators, have significant negative effects, tend to form insoluble precipitates with phytic acid and oxalic acid, which affect the intestinal absorption of iron ions and are prone to inflammation of the intestinal tract[7]. It have been reported that peptides extracted from oyster[7], Alaska pollock frames[8], and duck egg white[9] chelated with iron ions and formed peptide-iron complexes, which were not only effective in improving effects against IDA, but also had more impressive effects in promotion of iron absorption in human GI tract than iron sulphate.

Marine organisms contain abundant excellent proteins, and the biologically functional peptides extracted from them have great potential for application in functional foods[10]. Moreover, marine food-derived peptides have been shown to exhibit strong chelating ability for metal elements, which can significantly improve the bioavailability of metal ions. For example, sea cucumbers[11], oysters[7], Antarctic krill[5], and other marine organisms are abundant in proteins and have plentiful quantities of metal chelating amino acids, which have good metal chelating potential. *Mytilus edulis* is a typical marine bivalve mollusk, which is not only rich in protein and eight essential amino acids[12], but also has medicinal values such as nourishing the liver and kidney and regulating blood pressure, making it a nutritious marine organism[13]. However, currently there is little available research on *M. edulis* proteins as sources of food to act as raw materials for metal ion chelating peptides.

In this study, *M. edulis* protein hydrolysate (MEPH) was used as a raw material to prepare peptide-iron (MEPH-Fe) complexes by reacting with iron ions. The chelating conditions, the chelating properties, the GI digestion stability and the microstructure of the MEPH-Fe complexes have been investigated. Moreover, *in vivo* experiments on the protective effect of MEPH-Fe complexes against IDA were conducted in animal models of mice, hematological and organ indices and antioxidant capacity were measured, and the restorative effect on colonic inflammation was investigated. The results of this study were informative for the study of MEPH-Fe complexes as an iron supplement.

2. Materials and methods

2.1 Materials

M. edulis were purchased from a local market (Dalian, China). Alkaline protease (200 000 U/g) was provided from Nanning Pangbo Biological Engineering Co., Ltd. (Nanning, China). Ferrozine was purchased from Sangong Bioengineering Co., Ltd. (Shanghai, China). Iron (II) sulfate heptahydrate was purchased from the Tianjin Guangfu Fine Chemical Research Institute (Tianjin, China). Ascorbic acid was purchased from Shanghai Aladdin Biochemical Technology Co., Ltd. (Shanghai, China).

2.2 Preparation of the MEPH and MEPH-Fe complexes

The *M. edulis* were first shelled, the meat was removed and cleaned, then freeze-dried to remove moisture, finally ground into the powder. The *M. edulis* powder was dissolved in deionized water, stirred well and alkaline protease (200 000 U/g) was added, then the pH was adjusted to 9 and the reaction was carried out at 45 ℃ for 4 h. At the end of the reaction, the samples were inactivated in boiling water for 10 min. The reaction system was cooled and anhydrous ethanol was added until the concentration of anhydrous ethanol was 80% (*V*/*V*). The purpose of adding ethanol was to precipitate proteins and polysaccharides with higher molecular weights to improve the purity of the peptides. The reaction system was left to sediment for 24 h at 4 ℃. The system was then pump-filtered and rotary evaporated at 50 ℃ until the anhydrous ethanol was completely removed, and the remaining liquid was lyophilized as MEPH. According to the ratio of weight of lyophilized powder of MEPH and *M. edulis* protein, the yield of MEPH was about nearly 70%. MEPH was stored at –20 ℃ for subsequent experiments.

To produce the MEPH-Fe complexes with the highest iron-chelating rate, the reaction conditions, including the concentration of MEPH, reaction time, and temperature, were determined based on the results of the iron-chelating capacity. Once the optimal reaction conditions were established, the MEPH-Fe complexes was obtained by reacting the MEPH solution with iron (II) sulfate heptahydrate solution, followed by lyophilization.

2.3 Measurement of the iron-chelating capacity of MEPH

The ability of MEPH to chelate iron was measured by one of the methods used in the past, with a few modifications[14]. Under certain conditions, 1 mL of MEPH solution was reacted with 500 μL of iron (II) sulfate heptahydrate solution (2 mmol/L) (containing ascorbic acid 1% (*m*/*V*)), followed by the addition of 100 μL of ferrozine solution (0.01 mol/L). The main purpose of adding ascorbic acid was to inhibit the oxidation of Fe^{2+} in the liquid reaction system. At the end of the reaction, the OD value of the samples at 562 nm was measured using an enzyme marker (Infinite F200 PRO, Tecan, Männedorf, Switzerland) and the iron-chelating capacity was determined by the change in OD value. The iron-chelating capacity was determined by the following equation:

$$\text{Iron-chelating capacity (\%)} = \frac{OD_{blank} - OD_{sample}}{OD_{blank}} \times 100 \quad (1)$$

Where the blank samples were simply deionized water and ferrous sulfate solution.

2.4 Analysis of the amino acid composition of MEPH

MEPH (200 mg) was hydrolyzed by adding 3 mL sulfuric acid (6 mol/L) at 110 ℃ for 24 h, and then was volume-determined

to 25 mL with deionized water. A total of 1 mL of the sample was spin-dried and then 1 mL of concentrated hydrochloric acid (0.02 mol/L) was added to dissolve it, and then mixed and passed through the membrane. The sample was taken as 50 μL in an injection bottle and was measured by an amino acid analyzer (LA8080, Hitachi, Tokyo, Japan).

2.5 Fourier transform infrared (FTIR) spectroscopy analysis

Lyophilized powders of MEPH (1 mg) as well as MEPH-Fe complexes (1 mg) were taken and the samples (MEPH and MEPH-Fe complexes) were mixed with dried KBr (99 mg) and pressed. The spectra were examined by FTIR spectrometer (Spectrum Two, PerkinElmer, USA) and the spectra were measured in the range of 4 000–400 cm^{-1}.

2.6 Circular dichroism (CD) analysis

The CD spectra at 190-260 nm were measured using the CD spectrophotometer (J-1500, Jasco Corporation, Tokyo, Japan) by taking the same concentration (0.75 mg/mL) of MEPH and MEPH-Fe complexes in solution.

2.7 Ultraviolet-visible absorption spectroscopy

Equal amounts of MEPH and MEPH-Fe complexes (0.125 mg/mL) were dissolved in deionized water. The spectra of the 2 samples were then measured separately in the wavelength range of 190–450 nm using a UV-Vis spectrophotometer (Lambda 35, PerkinElmer, USA).

2.8 Fluorescence spectroscopy analysis

Fluorescence spectra of MEPH and MEPH-Fe complexes (0.642 mg/mL) were analyzed using the fluorescence spectrophotometer (F-2700, Hitachi High-Tech, Tokyo, Japan). The excitation and emission wavelengths were set at 280 and 290–500 nm, respectively, and the slit width was set at 5 nm and the photomultiplier voltage was set at 700 V during the measurement.

2.9 X-ray diffraction (XRD) analysis

The XRD spectra of MEPH, MEPH-Fe complexes (amounts required by equipment) and ferrous sulfate were determined using X-ray diffractometer (XRD-7000S, Shimadzu, Japan). The detailed experimental conditions were as follows: The scanning angle (2θ) ranged from 10° to 70° and the scanning speed was 5°/min.

2.10 Thermogravimetry-derivative thermogravimetry (TG-DTG) analysis

The thermal properties of MEPH and MEPH-Fe complexes (powder, 5 mg) in air at a rate of 10 ℃/min in the range of 50–500 ℃ were studied using the thermogravimetric analyzer (TA-Q500, TA Instruments,USA). An empty plate was used for comparison.

2.11 Simulated GI digestion experiment

The simulation of GI digestive process was done with some modifications based on the relevant literature[15]. The artificial gastric fluid was firstly water-bathed at 37 ℃ for 15 min, and then MEPH-Fe complexes and ferrous sulfate were added separately (Shanghai Yuanye Bio-Technology Co., Ltd., Shanghai, China). Samples were taken every 30 min during the gastric digestion stage. At the end of gastric digestion, the pH was adjusted to 6.8, and then the artificial small intestine fluid was added. Samples were taken at 30 min intervals during the intestinal digestion stage, respectively. After each sample, the enzyme was inactivated by heating at 95 ℃ for 15 min. being collected Then 10 000 ×g centrifugation was performed for 10 min. The supernatant was collected and the iron content was determined by atomic absorption spectrophotometer (ZA3000, Hitachi, Ltd., Tokyo, Japan). Iron solubility was calculated as follows:

$$\text{Iron solubility (\%)} = \frac{\text{Iron in supernatant (mg)}}{\text{Total iron in solution (mg)}} \times 100 \quad (2)$$

2.12 Determination of particle size distribution and Zeta potential

Particle size distribution and Zeta potential of MEPH and MEPH-Fe complexes were determined by a particle size and zeta potential analyzer (Zetasizer Nano-ZS, Malvern, UK) in 3 determinations at equal concentrations.

2.13 Scanning electron microscopy (SEM) analysis

The microstructures of the MEPH and MEPH-Fe complexes were observed by an SEM equipped with an Oxford Instruments X-Max50 energy-dispersive spectrometer (EDS) (JSM-7800F, Japan). Sample images were observed and surface elemental composition was determined at different magnifications.

2.14 In vivo protective effects of the MEPH-Fe complexes against IDA in mice

2.14.1 Animals and diets

The animal experiments were approved by the Animal Ethical and Welfare Committee of Dalian Polytechnic University (DLPU2024022). Male Kunming (KM) mice, aged 3 weeks, were obtained from Liaoning Changsheng Biotechnology Co., Ltd. (Shenyang, China). The mice were housed in a temperature-controlled room with a 12-h light and 12-h dark cycle, and they had access to adequate supply of water. Following a 48-h acclimatization period, 10 mice were randomly selected to serve as the control group and were fed with standard diets containing 45 mg/kg of iron. The remaining 50 mice were fed iron-deficient diets containing 5 mg/kg of iron for 15 days to establish the IDA model. After this period, blood samples were collected from the mice raised on iron-deficient chow, and the hemoglobin (Hb) content in their blood was measured using a kit (Nanjing Jianjian Bioengineering Institute, Nanjing, China). IDA was defined as a Hb content of less than 100 g/L. The IDA mice were then randomly divided into 5 groups, each consisting of 10 mice.

Model group: iron-deficient diet; $FeSO_4$ group: iron-deficient diet + ferrous sulfate (Fe^{2+}: 2 mg/kg); MEPH-Fe-low (MEPH-Fe-L) group: iron-deficient diet + MEPH-Fe complexes (Fe^{2+}: 1 mg/kg); MEPH-Fe-medium (MEPH-Fe-M) group: iron-deficient diet + MEPH-Fe complexes (Fe^{2+}: 2 mg/kg); MEPH-Fe-high (MEPH-Fe-H) group: iron-deficient diet + MEPH-Fe complexes (Fe^{2+}: 4 mg/kg). Based on the screening of chelating conditions conducted in the previous stage, an equivalent amount of MEPH was administered to all three doses of MEPH-Fe complexes, ensuring that the chelating rate of MEPH-Fe-M reached its maximum value. Then, based on the maximum iron-chelating capacity, the dosage of MEPH in *in vivo* experiments was meant to be capable of carrying the iron amounts corresponding to the necessary iron intake every day. Therefore, the calculation of the optimal chelation rate indicated that the gavage amount of MEPH for mice was 16.07 mg/100 g body weight (BW) in MEPH-Fe-M group. Additionally, both low-dose and high-dose groups were established to investigate the effects of varying doses of the MEPH-Fe complexes with the same amounts of MEPH but different amounts of iron ions as medium group. The mice were kept by gavage once a day for three consecutive weeks and their body weights were measured weekly.

2.14.2 Measurement of hematological indices in mice

At the end of the experiment, the mice were fasted for 12 h, and then blood samples were collected. Part of the collected blood samples were put into anticoagulation tubes for routine blood tests, and the remaining blood samples were centrifuged in centrifuge tubes. The separated serum was stored at –80 °C for subsequent experiments. Serum iron (SI) levels and total iron binding capacity (TIBC) were determined separately in each group of mice using kits (Nanjing Jiancheng Bioengineering Institute, Nanjing, China).

2.14.3 Organ coefficient

Mice were dissected and heart, liver, spleen and kidney were removed and immediately weighed. The organ coefficients were obtained by the following formula:

$$\text{Organ coefficient (g/100 g)} = \frac{\text{Organ weight}}{\text{Mouse body weight}} \times 100 \quad (3)$$

2.14.4 Iron content in organs

The livers, kidneys, and spleens of mice were weighed to specific weights, digested with concentrated sulfuric acid (18 mol/L), and then the concentration of iron ions was measured using an inductively coupled plasma emission spectrometer (Optima 8000, PerkinElmer, USA). The iron content in organs was calculated by using the following formula:

$$\text{Iron content in organs (mg/kg)} = \frac{C \times f \times V}{m} \quad (4)$$

In the formula, C (mg/L): the concentration of the solution element obtained from the test; f: the number of times the sample was diluted; V (L): the volume in which the sample was digested and fixed; m (kg): the mass of the organ weighed.

2.14.5 Antioxidant indicators in organs

Reduced glutathione (GSH), malondialdehyde (MDA), superoxide dismutase (SOD), and catalase (CAT) levels were measured according to the kit instructions (Nanjing Jiancheng Bioengineering Institute, Nanjing, China).

2.14.6 Determination of inflammatory cytokines

TNF-α and IL-10 in mice colon tissue were determined using ELISA kits (Shanghai ZCIBIO Technology Co., Ltd., China).

2.14.7 Histological analysis

The colon tissues were first immersed in 4% paraformaldehyde fixative overnight, then the fixed tissue blocks were dehydrated, cleared, wax impregnated, paraffin embedded, and prepared into 5 μm thick serial sections, which were finally stained with hematoxylin and eosin (H&E). The stained sections were observed using a biological microscope at different magnifications.

2.15 Statistical analysis

The experimental data were expressed as mean ± standard deviation (SD). SPSS 27.0 (IBM Co., Armonk, NY, USA) was used for statistical analysis. Comparisons between 2 groups were performed using Student's *t*-test, while differences among multiple groups were analyzed by one-way analysis of variance (ANOVA) followed by Duncan's multiple comparison test. Differences between groups were considered statistically significant at $P < 0.05$.

3. Results and discussion

3.1 Preparation of MEPH and MEPH-Fe complexes

Since alkaline protease-treated extracted proteins are more susceptible to hydrolysis and yield better contents of small peptides, alkaline protease was used in this study to obtain MEPH by hydrolyzing the proteins extracted from *M. edulis*[16]. In order to prepare MEPH-Fe complexes under optimal conditions, the effects of concentration of MEPH, chelating temperature and chelating time on the value of iron-chelating capacity were investigated. As shown in Fig. 1A, the iron-chelating capacity of MEPH initially increased in a dose-dependence manner, but stabilized after the MEPH concentration reached 4.5 mg/mL, finally reaching 91.99% at a concentration of 5 mg/mL. There was no significant difference ($P > 0.05$) on value of iron-chelating capacity between groups of 4.5 and 5.0 mg/mL, suggesting that the binding capability of iron ions had limits in this circumstance without permanent increase. Similar tendency was also observed for the chelating ability of bovine bone collagen peptides with calcium ions where there was no significant change in calcium ion chelating capacity when the peptide/calcium ratio was between 3:1 and 5:1[17]. The effects of chelating temperature on the iron-chelating capacity of MEPH were also investigated. The results in Fig. 1B showed that the values of iron-chelating capacity gradually increased from 35 to 45 ℃ and become steady afterwards. The reactivity of iron ions is temperature dependent, and the

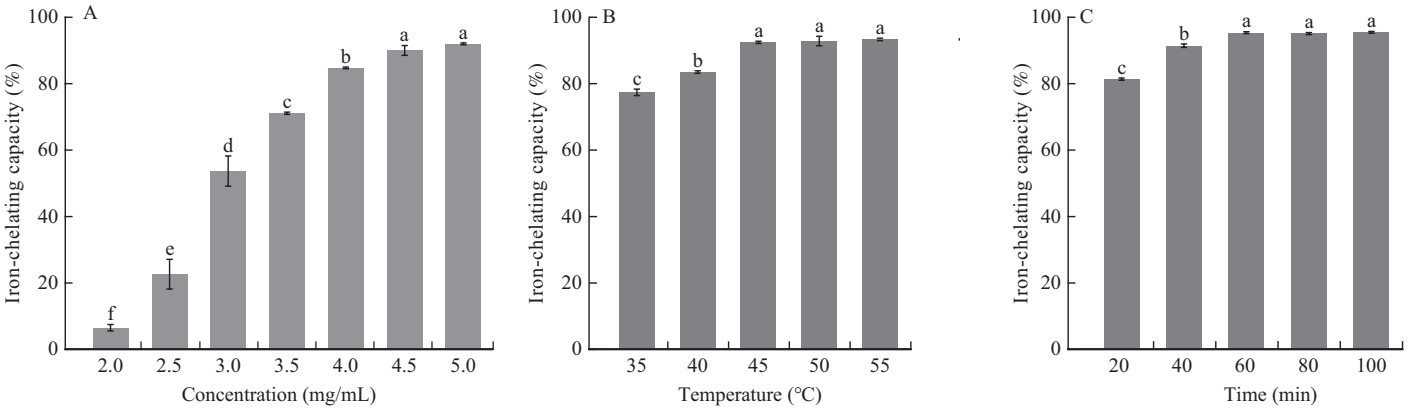

Fig. 1 Determination of iron-chelating capacity of MEPH. (A) Iron-chelating capacity of MEPH on indicating concentrations (2.0, 2.5, 3.0, 3.5, 4.0, 4.5, 5.0 mg/mL). (B) Iron-chelating capacity of MEPH at temperature of 35, 40, 45, 50 and 55 ℃. (C) Iron-chelating capacity of MEPH on time of 20, 40, 60, 80 and 100 min. Different letters above the bars indicated significant differences among groups ($P < 0.05$).

appropriate temperature accelerates the movement of the molecules, leading to accelerated rates of chelation reactions[18]. In addition, the reaction temperature should be low as much as possible since high temperature would result in the oxidation of divalent iron ions and negatively influence the biological effects of MEPH-Fe complexes[19]. Similarly, as shown in Fig. 1C, the values of iron-chelating capacity increased significantly in a time-dependent manner and remained stable after incubation time of 60 min. Therefore, the concentration of MEPH was chosen to be 4.5 mg/mL, and the reaction conditions were 45 ℃ for 60 min for the subsequent experiments. Moreover, the stability of MEPH-Fe complexes was also essentially important in this study. The MEPH-Fe complexes utilized in this research were freshly synthesized for each individual experiment, encompassing both characterization processes and the experiments involving mice. On the other hand, the MEPH-Fe complexes were stored in powdered form where the MEPH-Fe complexes samples contained ascorbic acid to maintain the divalent form of iron. The only circumstance in which the MEPH-Fe complexes were susceptible to stability or oxidation issues was when it was in liquid form (dissolved in water). To evaluate the stability of the MEPH-Fe complexes in this state, the samples were dissolved in distilled water and stored at 4 ℃ for a duration of 7 days (Fig. S1). The results indicated that, during the storage period, no significant color changes or precipitation were observed in the samples, demonstrating that both the divalent iron and MEPH-Fe complexes remained stable at 4 ℃.

3.2 Characterization of conformational properties of MEPH and MEPH-Fe complexes

Amino acids in peptides (tryptophan, phenylalanine and tyrosine) produce endogenous fluorescence at specific wavelengths. The interaction between the metal ions and the organic ligand groups can be effectively reflected by the change of fluorescence intensity[7]. As shown in Fig. 2A, the results indicated that the fluorescence emission peaks of MEPH and MEPH-Fe complexes were shown at 366 and 363 nm, respectively, and the intensity of the peaks of MEPH decreased from 1 730 to 1 218 after chelation with iron ions, indicating that the fluorescence quenching occurred after chelation with iron ions. The reasons for such a significant shift might be considered as follows: 1) the reaction of the chromophore with iron ions formed a new structure, leading to changes in the energy of the excited state and thus reduced the fluorescence intensity; 2) iron ions induced peptide folding and fluorescence quenching of MEPH and resulted in altered peptide conformation and reduced fluorescence intensity[20]. Endogenous fluorescence had also been reported to be significantly reduced by the addition of $CaCl_2$ to fish bone collagen peptides[21].

UV-Vis spectroscopy is commonly used to analyze the structural characteristics of substances, especially in the formation of complexes between metal ions and organic ligands that produce new absorption peaks or shifts[22]. The UV-Vis absorption spectra of MEPH and MEPH-Fe complexes were shown in Fig. 2B. Compared with MEPH alone, the MEPH-Fe complexes showed a significant shift in the absorption peak around 270 nm, suggesting that aromatic amino acid residues might be involved in the chelation of MEPH with iron ions, such as tryptophan, tyrosine and phenylalanine. The peptide extracted from sea cucumber was also reported to show ultraviolet shift when chelated with zinc ions, proving that the extracted peptide has good chelating ability with zinc ions[11]. Based on the shift of UV-Vis spectra, it was highly inferred that the MEPH successfully bound with iron ions and formed MEPH-Fe complexes.

CD spectroscopy is a sophisticated method for studying the secondary structure of proteins and peptides. As shown in Fig. 2C, the addition of iron ions resulted in the disappearance of α-helix and the decrease of the content of β-turn from 35.53% to 24.10% in the MEPH-Fe complexes. The content of β-sheet increased from 22.27% to 30.20%, and the content of random coil was increased from 40.07% to 45.70%. These results suggest that iron ions might have mainly induced the structural transition of MEPH from α-helix and β-turn to β-sheet. In addition, the incorporation of iron ions induced peptide folding and the formation of more compact secondary structures[23]. Similarly, it was found that calcium induced a structural shift in herring egg phosphopeptides from α-helix and β-turn to β-sheet[24].

When metal ions bind to ligand of peptides that contains atoms such as O, N, and S, the absorption peaks in the infrared spectrum usually change due to the vibration of the ligand bonds[25]. Thus, the interaction of iron ions with the organic groups of MEPH could be characterized and revealed. As shown in Fig. 2D, the amide A bands of MEPH and MEPH-Fe complexes were located at 3 378 and 3 377 cm^{-1}, respectively, and were attributed to the stretching vibration of the N—H bond. The vibrational spectral regions of 1 700–1 600

and 1 600–1 500 cm^{-1} correspond to the stretching vibrations of the amide I and amide II bands, respectively[17]. The absorption band of MEPH at 1 631 cm^{-1} was characterized as the amide I band, which was associated with the stretching vibration of the carbonyl group (C=O) of the amide (peptide bond). The absorption band of MEPH at 1 517 cm^{-1} was characterized as the amide II band from the coupling of the C—N stretching vibration and the N—H bending vibration. When the MEPH-Fe complexes were formed, the amide I and amide II bands shifted to the higher frequency region to 1 632 and 1 518 cm^{-1}, respectively. The position of the C—O stretching vibration peak in the carboxylate group was usually in the range of 1 000–1 300 cm^{-1}, and the absorption peak shifted from 1 040 to 1 042 cm^{-1} upon the formation of the MEPH-Fe complexes. Therefore, it was hypothesized that MEPH binds to ferrous ions through the amino and carboxyl groups of the peptide chain and the peptide bond[26].

XRD could reflect the complexes formed between organic ligands and metal ions by the diffraction peaks, peak intensities and peak position changes of the sample[17]. As shown in Fig. 2E, many crystal diffraction peaks in the diffractograms of ferrous sulfate could be found, while the diffractograms of the MEPH and MEPH-Fe complexes had no obvious crystal diffraction peaks, indicating that the crystal-associated signals of ferrous sulfate were completely covered

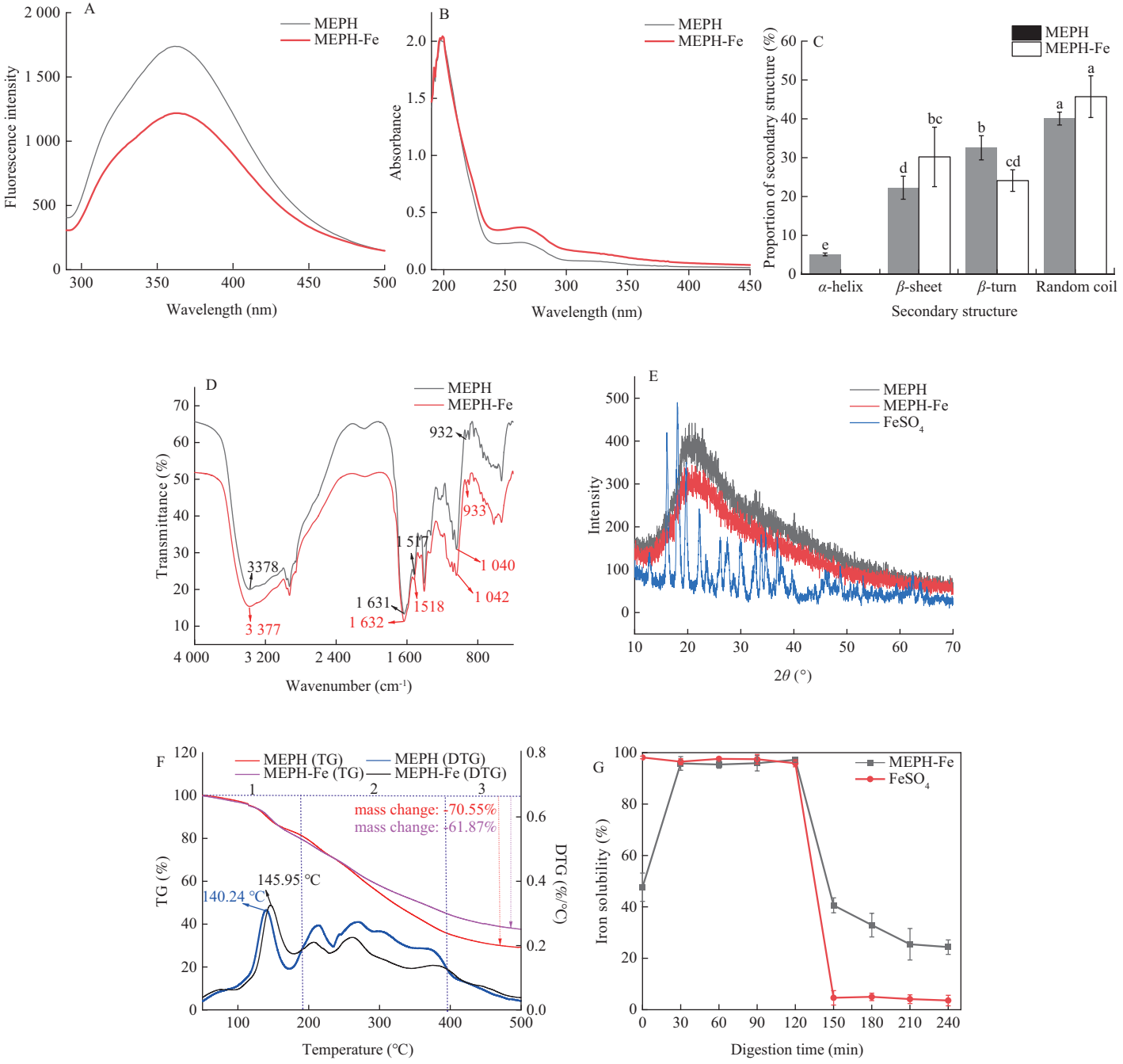

Fig. 2 Characterization of MEPH-Fe complexes. (A) Fluorescence spectrum of MEPH and MEPH-Fe complexes. (B) UV-Vis spectrum of MEPH and MEPH-Fe complexes. (C) Quantification of secondary structures of MEPH and MEPH-Fe complexes. (D) The FTIR spectra of MEPH and MEPH-Fe complexes. (E) XRD patterns of MEPH and MEPH-Fe complexes. (F) TG-DTG diagram of MEPH and MEPH-Fe complexes. (G) Iron solubility of MEPH-Fe complexes and $FeSO_4$ under simulated digestion. Different letters above the bars indicate significant differences among groups ($P < 0.05$).

by chelation by MEPH. Moreover, compared with the MEPH, the intensity of the diffraction peaks of the MEPH-Fe complexes decreased, indicating that MEPH and ferrous sulfate were not simply mechanically mixed, but the new chemical complex formed between them[27].

The thermal stability of MEPH and MEPH-Fe complexes was determined by TG-DTG as shown in Fig. 2F. The weight of MEPH decreased by 70.55% during the temperature increase from 50 to 500 ℃, while the weight of MEPH–Fe complexes decreased by 61.87%. The whole thermal decomposition process was mainly divided into two stages, which were stage 1: water loss, and stage 2: thermal degradation. In stage 1, the initial degradation temperature of MEPH was 140.24 °C, which was mainly attributed to the evaporation of absorbed water, while the initial degradation temperature of MEPH-Fe complexes was 145.95 °C. Subsequently, in phase 2, which included the disruption of peptide bonds (progressive deamination, decarboxylation and depolymerization) at various sites of MEPH, the thermal degradation rate of MEPH was observed to be higher than that of the MEPH-Fe complexes. The results suggested that the MEPH-Fe complexes were more stable substance with higher thermal stability compared to MEPH, which may be mainly due to the fact that more energy was required for the breakage of the ligand bond formed between MEPH and iron ions.

In the GI environment, several factors, such as the pH and various proteases, could affect the solubility and bioavailability of iron supplements[28]. Consequently, it was essential to investigate the solubility of MEPH-Fe complexes and to compare them with ferrous sulfate. The solubility of MEPH-Fe complexes and ferrous sulfate in a simulated GI environment was illustrated in Fig. 2G. The results clearly indicated that the concentration of iron ions in the ferrous sulfate group remained stable, consistently exceeding 95% for the first 120 min, before rapidly declining to nearly 0% between 120 and 150 min. This suggested that iron ions maintained high solubility during the gastric phase (characterized by low pH) but were inevitably consumed by precipitation during the intestinal phase (characterized by high pH). In contrast, the solubility of MEPH-Fe complexes increased gradually during the gastric digestion phase, rising from 47.67% to 95.83%. This indicated that the adaptation of iron loaded in MEPH-Fe complexes to the gastric phase occurred progressively. Upon entering the intestinal digestion stage, the solubility of iron ions in the MEPH-Fe complexes exhibited a significantly reduced decline in solubility compared to the ferrous sulfate group. This phenomenon can be attributed to the interaction of dietary components, such as tannins, phytates, and dietary fiber, with iron ions in the GI tract, leading to precipitation and ultimately resulting in reduced bioavailability of the mineral salts[29]. However, MEPH-Fe complexes reduced the precipitation of iron ions by competitive effects against precipitation and increased the absorption of iron ions by maintaining the soluble form. The results demonstrated that MEPH-Fe complexes were more stable in the simulated *in vitro* GI environment compared to ferrous sulfate[30].

Among the structural information of peptides affecting the chelating ability of iron ions, the amino acid composition plays an important role because of the differences in the binding affinity of various kinds of amino acids for iron ions[7]. As shown in Table 1, the 2 amino acids with the highest MEPH content were glutamic acid and aspartic acid, which were significantly higher than the other amino acids, accounting for 13.78% and 12.67%, respectively. The next highest contents were alanine, arginine, and phenylalanine, which were close to each other with 6.78%, 6.68%, and 6.63%, respectively. Aspartic acid and glutamic acid have also been reported to be the major amino acids in Antarctic krill hydrolysates[5]. Both aspartic acid and glutamic acid contained 2 carboxyl groups and one amino group, and combined with the results of FTIR spectroscopy, it was hypothesized that the carboxyl groups as well as the amino groups in glutamic acid and aspartic acid in MEPH were involved in the chelation reaction. Heptapeptide, abundant in aspartic acid and glutamic acid, has been reported to have excellent calcium-binding activity, which enhances calcium absorption[31].

Table 1
Amino acid composition of MEPH.

Amino acids	Absolute content (mg/g)	Relative content (%)
Glutamic acid	109.78 ± 0.09	13.78 ± 0.05
Aspartic acid	100.92 ± 0.18	12.67 ± 0.04
Alanine	53.97 ± 0.63	6.78 ± 0.05
Arginine	53.25 ± 1.10	6.68 ± 0.11
Phenylalanine	52.83 ± 0.27	6.63 ± 0.04
Threonine	49.32 ± 0.15	6.19 ± 0.02
Lysine	48.63 ± 0.30	6.11 ± 0.01
Glycine	48.28 ± 0.15	6.06 ± 0.01
Tyrosine	48.05 ± 0.60	6.03 ± 0.05
Leucine	47.48 ± 0.42	5.96 ± 0.03
Valine	45.42 ± 0.28	5.70 ± 0.03
Serine	43.66 ± 0.26	5.48 ± 0.01
Proline	27.21 ± 1.39	3.42 ± 0.19
Isoleucine	24.55 ± 0.34	3.08 ± 0.03
Histidine	21.08 ± 0.33	2.65 ± 0.03
Methionine	14.75 ± 0.07	1.85 ± 0.01
Cystine	7.31 ± 0.15	0.92 ± 0.02

3.3 Determination of structural and morphological properties of MEPH and MEPH-Fe complexes

The results of the particle size distribution of the MEPH and MEPH-Fe complexes determined by nanoparticle sizer were shown in Fig. 3A. Based on the diagram of results, the particle size distribution of the MEPH was mainly divided into two peaks located at 108 and 893.8 nm, respectively, where the particle size distribution of the MEPH-Fe complexes obviously enhanced and mainly divided into 2 peaks at 197.6 and 2 211 nm. The results showed that the particle size of MEPH was significantly lower than that of MEPH-Fe complexes, which also provided evidence for the interaction between iron ions and MEPH. It was hypothesized that the increase in MEPH-Fe complexes particles may be due to the fact that iron ions trigger the aggregation of protein molecules by shielding the negative charges on the peptide chains and act as salt bridges between the negatively charged carboxyl groups on neighboring peptide molecules, thus inducing the transformation of peptide secondary structures[32]. Calcium has been reported to promote the formation of peptide β-sheet structures and induce the structural folding of peptides

to form spherical nanoparticles[24]. Combined with the above results of CD, it can be inferred that the formation of *β*-sheet is the possible reason for the larger particle size of the MEPH-Fe complexes. The interaction of Antarctic krill peptides with zinc ions has been reported to show similar results[33].

Zeta potential is a physicochemical indicator that reflects the charge state on the surface of particulate substances. As illustrated in Fig. 3B, all groups with increasing concentrations of MEPH exhibited negative Zeta potentials (less than –30 mV), suggesting that MEPH remained relatively stable in dissolving environments. Additionally, the absolute values of the Zeta potential increased in a dose-dependent manner as the concentrations of MEPH increased. Furthermore, in comparison to MEPH alone, the absolute values of the Zeta potentials for MEPH-Fe complexes decreased at the same concentration but remained above 30 mV. This indicated that iron ions neutralized the negative charges in the ligands of MEPH, such as carboxyl groups, while still maintaining dissolving stability during the chelation reaction[28]. As the increasing concentration of MEPH, the negative charges in MEPH accumulated probably due to the accumulation of negatively charged amino acids of MEPH. Therefore, in conjunction with the particle size distribution and Zeta potential results, it was hypothesized that iron ions may promote protein aggregation by shielding the negative charges on the MEPH chains and act as salt bridges, leading to increased particle size and decreased absolute values of Zeta potential[23].

The morphological features of the surfaces of MEPH and MEPH-Fe complexes were analyzed using SEM. As illustrated in Fig. 3C, MEPH exhibited spherical or spheroidal aggregates at magnifications of 2 000× and 1 000×, respectively (Figs. 3C_1 and C_3). In contrast, the MEPH-Fe complexes predominantly displayed irregular aggregates with rod-like and lamellar structures (Figs. 3C_2 and C_4). This difference was likely attributable to the carboxyl and amino groups in MEPH binding to iron ions, which facilitated the 'bridging role' that promoted protein aggregation and consequently altered the microscopic morphology[18]. Meanwhile, the elemental compositions of the MEPH and MEPH-Fe complexes were simultaneously determined using EDS, as shown in Figs. 3C_5 and C_6. There was almost no signal of iron in the EDS spectrogram of MEPH whereas the EDS spectrogram of MEPH-Fe complexes exhibited the signal of iron ion (3.42%), sideways proving the successful interactions of iron ions with MEPH and the formation of MEPH-Fe complexes[34].

3.4 Determination of ameliorative effects of MEPH-Fe complexes against IDA symptoms in mice

To investigate the effects of MEPH-Fe complexes on the recovery from IDA symptoms in mice, an IDA mouse model was established using an iron-deficient diet. Subsequently, 3 concentrations of MEPH-Fe complexes (low, medium, and high) were administered, with ferrous sulfate serving as a positive control. The recovery effects of the MEPH-Fe complexes on IDA symptoms were evaluated by measuring various biological indicators. The weekly body weights of the mice are presented in Fig. 4A. During the first 2 weeks of the IDA model, the control group exhibited significantly greater body weight gains compared to the model group ($P < 0.05$), indicating that iron deficiency may profoundly impact metabolism-related biological functions in IDA mice. Over the 3-week period of iron supplementation with these iron sources, the body weights of IDA mice treated with increasing doses of MEPH-Fe complexes and ferrous sulfate gradually approached those of the control group. Notably, the body weights of mice receiving MEPH-Fe complexes, particularly at the medium dose, demonstrated more effective recovery compared to those in the ferrous sulfate group. These findings suggested that MEPH-Fe complexes may positively influence the growth of IDA mice, as indirectly evidenced by weight gain[35]. Furthermore, the results of the organ coefficients, including heart, liver, spleen, and kidney of each group were shown in Figs. 4B-E. Compared with the control group, the heart, liver, spleen, and kidney of mice in the model group showed different degrees of hypertrophy, while the heart, liver, and spleen of IDA mice treated with the MEPH-Fe complexes were restored to the normal levels ($P < 0.05$). The Ejiao peptide-iron chelates were also reported to have good restorative effects on IDA-induced cardiac, hepatic, and splenic hypertrophy in mice[36]. And duck egg white peptide-ferrous chelate showed a similar trend in the recovery of renal hypertrophy[9]. Among them, it could be seen that the spleen was the most sensitive organ to iron deficiency. The spleen is the largest secondary lymphoid organ in the body and is essential for hematopoiesis and blood filtration[37]. Therefore, it was hypothesized that the enhanced splenic coefficient in the model group might be due to the aggregation of erythrocytes in the spleen and dilation of the splenic sinusoids.

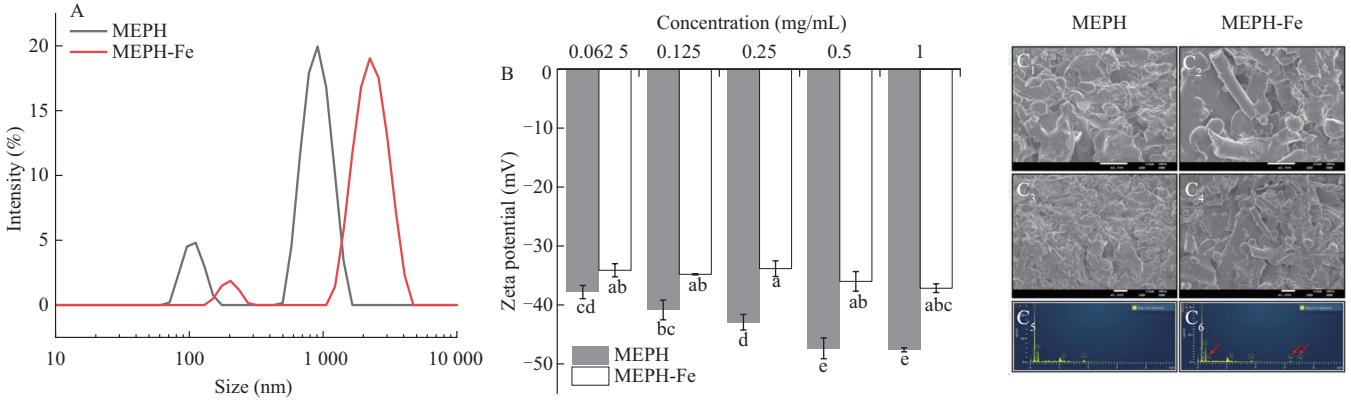

Fig. 3 Characterization of microstructures of MEPH-Fe complexes. (A) Particle size distribution of MEPH and MEPH-Fe complexes. (B) Zeta potential of MEPH and MEPH-Fe complexes at different concentrations. (C) Morphologic appearances of surfaces MEPH and MEPH-Fe complexes (C_1–C_4: SEM images; C_5–C_6: EDS images).

The SI and TIBC are significant indicators for the clinical diagnosis of IDA[35]. As shown in Fig. 4F, the result showed that the SI content in the model group was significantly lower than that in the control group ($P < 0.05$) while the results in Table 2 demonstrated that the hematological indices of the control group were significantly higher than those of the model group ($P < 0.05$), offering the direct evidence that the establishment of the IDA mice model with iron-deficient diet treatment was successful. The SI contents in the group of $FeSO_4$ and groups of the MEPH-Fe complexes was elevated compared with those in the model group where there was a significant difference between the MEPH-Fe-M group and the $FeSO_4$ group ($P < 0.05$), suggesting that the medium dose of MEPH-Fe complexes not only sufficiently approached the level of control group but also possessed significant recovery effects than ferrous sulfates. Similar results have been reported for Ejiao peptide-iron chelates[36]. As the level of hematological indices reflects the level of hematopoietic capacity, these indices were also measured to assess the recovery effect of MEPH-Fe complexes. On the other hand, compared with the model group, the hematological indices in all MEPH-Fe groups were significantly higher than that in model group; while the hematological indices in MEPH-Fe-M group were higher than that in model group, even though they were not statistically significant ($P > 0.05$), which was also similar to the experimental results of the Ejiao peptide-iron chelates[6]. Moreover, the results in Fig. 4G showed that the serum TIBC level was significantly higher in the model group than that in the control group ($P < 0.05$) while the capacity levels in both the group of $FeSO_4$ and each group of the MEPH-Fe complexes were restored to normal levels in comparison with the model group. The SI contents in the group of MEPH-Fe-M indicated that the amount of iron that could be absorbed by the organism was high, which indirectly indicated that compared with ferrous sulfate, the MEPH-Fe complexes were less likely to be precipitated in the GI tract and was more easily absorbed. Due to the low SI content, the transferrin bound to iron became less and the transferrin without iron increased, resulting in the enhancement of TIBC content in the model group. Compared with group of $FeSO_4$, it was hypothesized that the MEPH-Fe complexes were more easily absorbed by the organism and entered the bloodstream leading to an increase in the SI content of the mice and a restorative effect on the TIBC in the IDA mice. In summary, the MEPH-Fe complexes were effective in restoring the SI and TIBC levels against the iron deficiency-induced IDA in mice, where the medium dose of the MEPH-Fe complexes was proved to possess more effective iron absorption-promotive functionality compared with the addition of ferrous sulfates.

Table 2
Levels of RBC, HGB, HCT, MCV, MCH, and MCHC in mice.

	Control	Model	$FeSO_4$	MEP-Fe-L	MEP-Fe-M	MEP-Fe-H
RBC ($\times 10^{12}$/L)	10.50 ± 0.42^{a}	7.99 ± 0.21^{b}	10.78 ± 0.19^{a}	10.87 ± 1.28^{a}	11.03 ± 0.43^{a}	10.83 ± 0.21^{a}
HGB (g/L)	151.00 ± 4.00^{a}	87.00 ± 3.61^{b}	145.00 ± 2.00^{a}	135.33 ± 23.71^{a}	146.00 ± 6.56^{a}	152.67 ± 3.21^{a}
HCT (%)	48.33 ± 1.97^{a}	30.20 ± 0.82^{b}	47.80 ± 1.25^{a}	45.13 ± 7.41^{a}	49.50 ± 1.55^{a}	50.07 ± 1.05^{a}
MCV (fL)	47.03 ± 1.89^{a}	36.17 ± 1.38^{c}	43.70 ± 0.75^{b}	43.27 ± 2.06^{b}	44.33 ± 1.30^{ab}	45.40 ± 0.87^{ab}
MCH (pg)	14.2 ± 0.53^{a}	10.50 ± 0.75^{c}	12.97 ± 0.40^{b}	12.90 ± 0.70^{b}	13.17 ± 0.60^{ab}	13.90 ± 0.26^{ab}
MCHC (g/L)	307.33 ± 3.51^{a}	288.33 ± 5.51^{c}	303.33 ± 1.53^{ab}	301.00 ± 2.65^{b}	304.33 ± 0.58^{ab}	307.33 ± 1.53^{ab}

Notes: The levels of RBC, HGB, HCT, MCV, MCH and MCHC in mice *in-vivo*. Different letters in the table indicate significant differences between scores ($P < 0.05$), different numbers present for different indices.

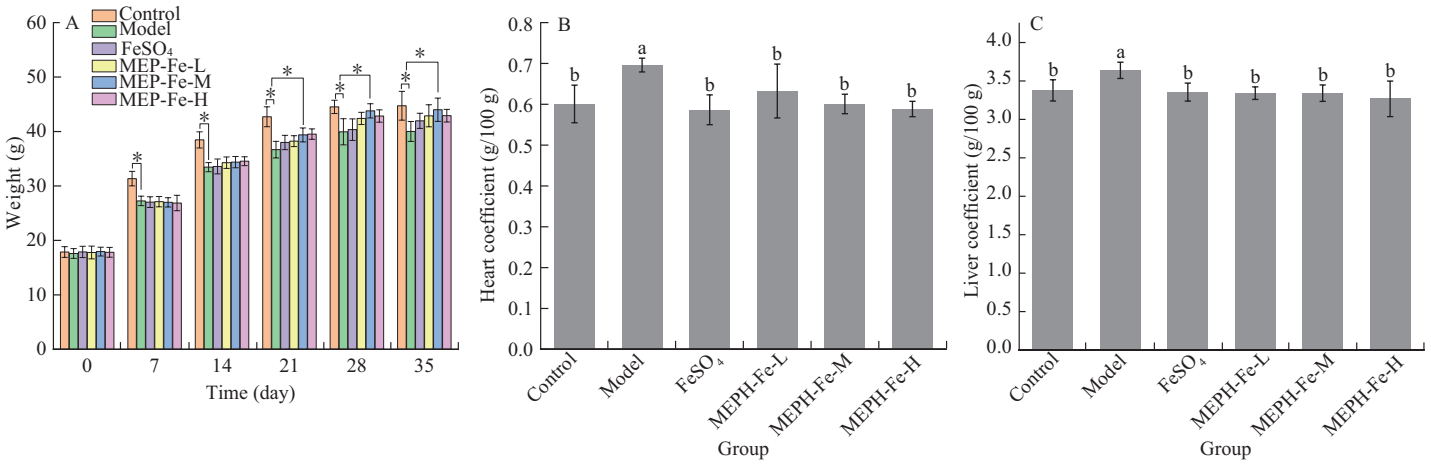

Fig. 4 (A) Body weight of mice on the indicating period. Organ coefficient and hematological indexes. (B) Heart coefficient. (C) Liver coefficient. (D) Spleen coefficient. (E) Kidney coefficient. (F) SI levels. (G) TIBC levels. *$P < 0.05$. Different letters above the bars indicate significant differences among groups ($P < 0.05$).

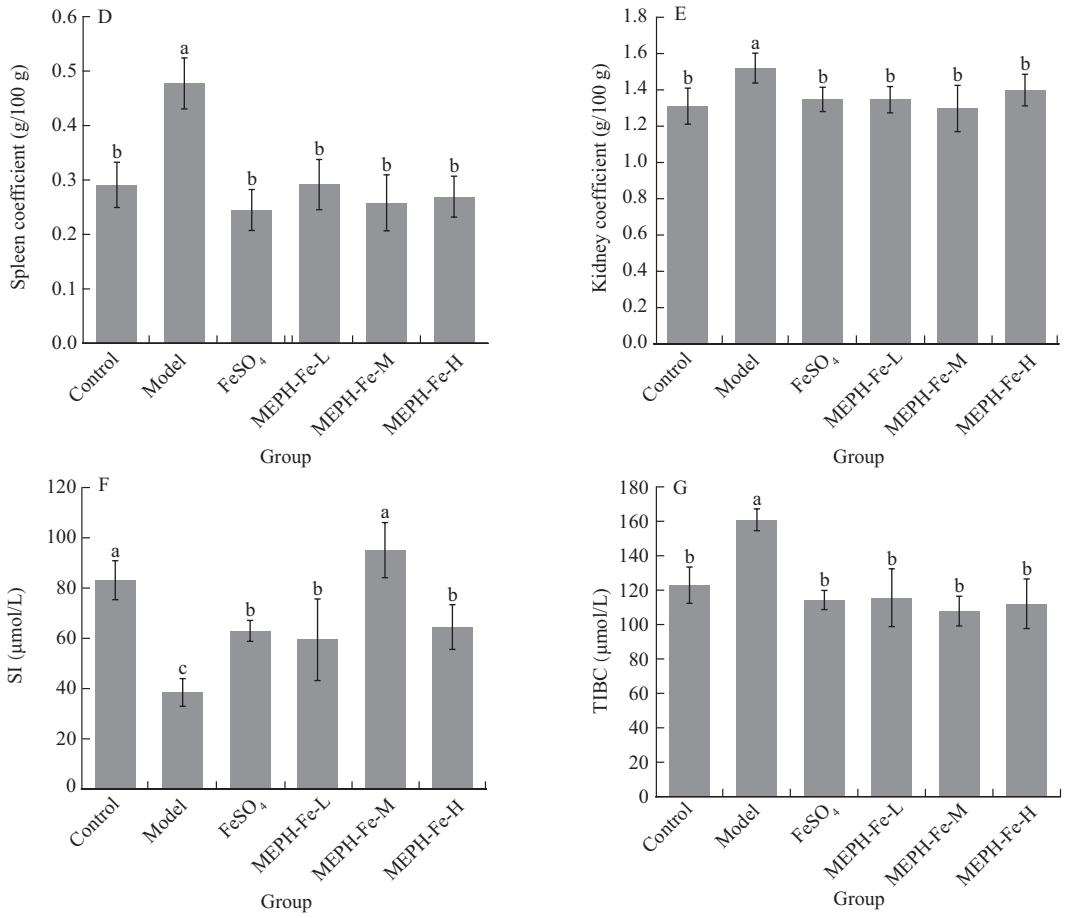

Fig. 4 (*Continued*)

3.5 Effects of MEPH-Fe complexes on iron distribution and oxidative stress in organs of IDA mice

The liver and spleen, the major iron storage tissues in the organism, perform vital roles in iron homeostasis. The organism can utilize iron stored in the liver and spleen for transport to maintain SI homeostasis[38]. The iron contents in liver, kidney and spleen after iron supplementation in each group were shown in Figs. 5A-C. The iron contents in the liver, kidney, and spleen of mice in the model group were significantly lower than those in the control group, which were consistent with the results of contents of SI above (Fig. 4F). Furthermore, it was obvious that of MEPH-Fe-M and MEPH-Fe-H groups exhibited significant enhancements of iron contents in these 3 organs compared with model group, and MEPH-Fe-H group was shown to be more effective than $FeSO_4$ group in restoring the iron contents in kidney and spleen ($P < 0.05$). Nanoliposome-embedded iron chelates showed comparable trends of contents iron ions in rat liver[39]. It was noteworthy that we found that values of iron contents in 3 organs treated by groups of MEPH-Fe-H seemed to be higher than those groups MEPH-Fe-M, but the group MEPH-Fe-M promoted higher SI value in mice (Fig. 4F) even though these two doses both exhibited impressive recovery effects. For now, the mechanism of transfer and transportation of peptide-metal complex across the intestinal membrane or their accumulations in vital organs were not fully understood. To our best knowledge, the peptide-metal complex could be directly absorbed through intestinal membrane without being totally decomposed by cellular environments, probably leading to remaining high amounts in the blood vessel. In addition, we hypothesized that the MEPH-Fe complexes in the vessel might also provide the properties of slow-release and attenuate the accumulations of iron in organs compared with free iron ions, since more free iron ions contained in MEPH-Fe-H group, which needs to be verified in the future work.

SOD and CAT are important antioxidant enzymes in living organisms and play important roles in regulating a variety of cellular functions and protecting cells from oxidative damage[41]. MDA is often used as the marker of oxidative stress[42], whereas GSH is one of the antioxidant peptides in organism, reflecting antioxidant capacity of the organism[35]. The antioxidant effects of MEPH-Fe complexes in mice were evaluated by the determination of these indices above. The SOD contents in kidneys of mice were shown in Fig. 5D. The SOD content in model group was significantly lower than that in control group ($P < 0.05$), indicating that the SOD activity significantly decreased in the kidneys in IDA mice. In contrast, the SOD content in the group of $FeSO_4$ and MEPH-Fe groups was significantly higher ($P < 0.05$), suggesting that the MEPH-Fe complexes were effective in restoring SOD contents in mice. In addition, there was no significant difference between the MEPH-Fe-L group and the $FeSO_4$ group, indicating that the low-dose of MEPH-Fe complexes was barely capable in restoring the SOD levels in IDA mice. However, SOD

content in MEPH-Fe-M group was significantly higher compared with $FeSO_4$ group ($P < 0.05$), indicating that the medium dose of the MEPH-Fe complexes had the strongest restorative effect on IDA-induced oxidative stress[38]. The GSH contents in liver and kidney of mice were illustrated in Figs. 5E and 5F, respectively. In both the livers and kidneys of the mice, the GSH levels in model group were significantly lower than those in the control group. In contrast, the $FeSO_4$ and MEPH-Fe complexes groups notably restored the GSH levels that had declined due to IDA, with MEPH-Fe-M group exhibiting the highest GSH content among all iron supplement groups. The MEPH-Fe complexes appeared to either slow down the depletion of GSH or promote its synthesis in the IDA-induced mice, restoring GSH levels in livers and kidneys to normal. Additionally, the MDA content in the liver of mice was also examined (Fig. 5G). Compared with the model group, all MEPH-Fe complexes groups exhibited significantly reduced MDA levels in the liver ($P < 0.05$). Furthermore, dysregulation of iron pathways can lead to cellular oxidative stress, primarily attributed to the generation of hydroxyl radicals and the initiation of lipid peroxidation, resulting in the formation of mutagenic byproducts such as MDA and causing

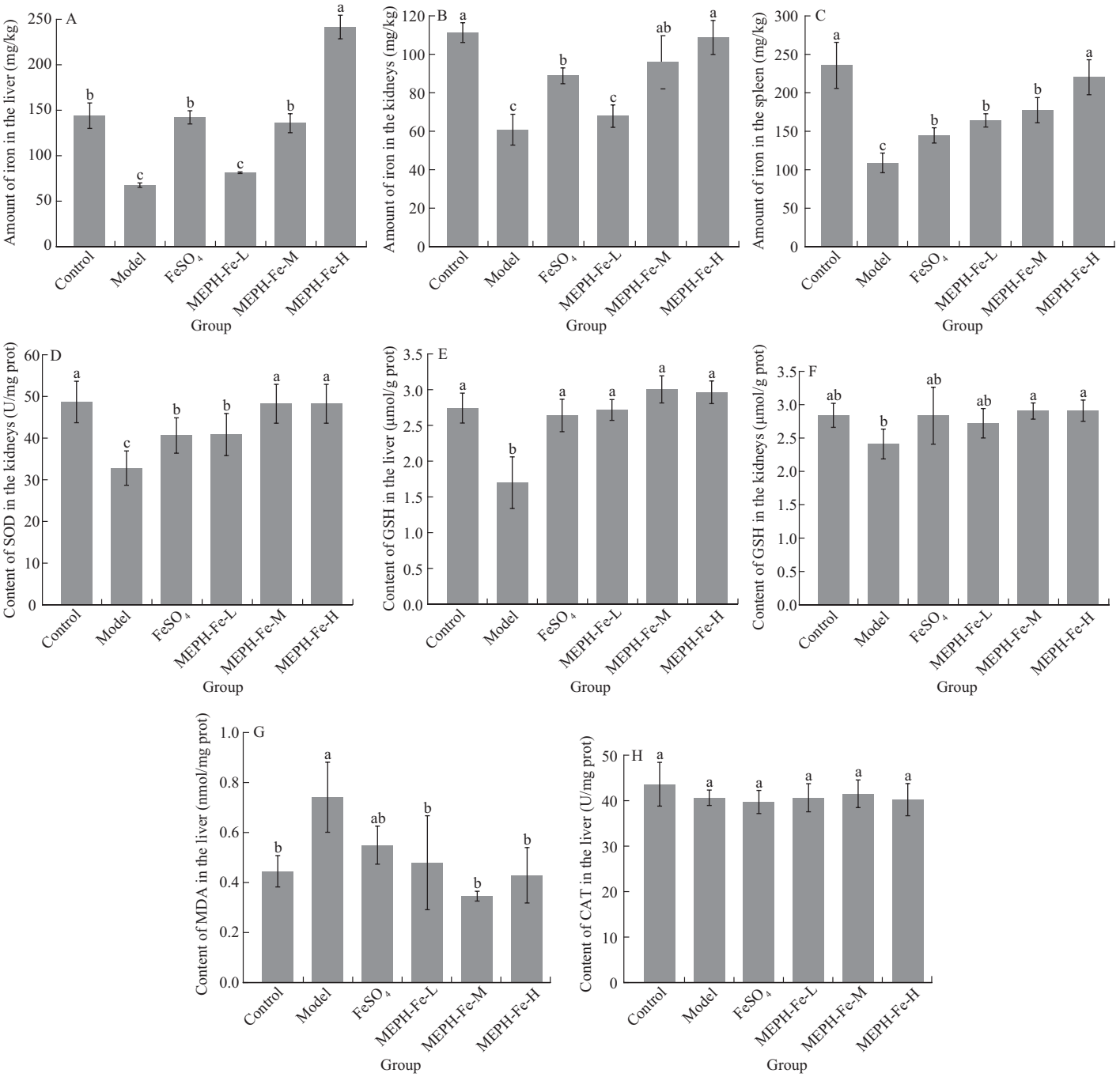

Fig. 5 Iron content in organs and indicators of oxidation: (A) Amount of iron in the liver. (B) Amount of iron in the kidneys. (C) Amount of iron in the spleen. (D) Content of SOD in the kidneys. (E) Content of GSH in the liver. (F) Content of GSH in the kidneys. (G) Content of MDA in the liver. (H) Content of CAT in the liver. Different letters above the bars indicate significant differences among groups ($P < 0.05$).

damage to cellular structures and functions[35]. Therefore, the MEPH-Fe complexes might be able to attenuate the oxidative stress-associated lipid peroxidation reaction in the livers and kidneys of IDA-induced mice as well. The CAT contents in the liver of mice were shown in Fig. 5H. The CAT content in model group was slightly lower than that in control group, and the CAT content in MEPH-Fe-M group tended to increase, but the difference was not significant ($P > 0.05$)[42]. In conclusion, MEPH-Fe complexes have significant antioxidant effects in IDA mice and has better positive effects than ferrous sulfate.

3.6 Recovery effects of MEPH-Fe complexes against iron deficiency-induced colonic inflammation in IDA mice

The colonic tissues in the IDA mouse model were stained with H&E to further investigate the effects of MEPH-Fe complexes on iron deficiency-induced intestinal inflammation. As shown in Fig. 6A, the colonic epithelial cells of control group were tightly and orderly arranged, exhibiting well-structured crypts, and a substantial number of goblet cells. In contrast, the colonic tissues of mice in model group displayed severe damage, characterized by infiltration of inflammatory cells into the intestinal tissues, elongated crypts, and a significant reduction in the number of goblet cells. However, these adverse effects were markedly alleviated in mice treated with various MEPH-Fe complexes formulations, particularly in MEPH-Fe-L and MEPH-Fe-M groups. Additionally, the MEPH-Fe-H and $FeSO_4$ groups were less effective in ameliorating the inflammation of colonic tissues, exhibiting notable inflammatory symptoms. It was posited that the overload of free iron ions may lead to iron deposition in the intestinal mucosa, thereby exacerbating inflammation by disrupting intestinal mucosal homeostasis[43]. In this study, not only the group of ferrous sulfate but also the high content of MEPH-Fe complexes contained excessive free iron ions, leading to increased oxidative stress in intestinal tissues even though they also could offer good bioavailability of iron. Meantime, the Ejiao peptide-iron chelates had similar results for colon recovery in regulating IDA in mice based on the previous reports[6].

The next study was to observe the effect of MEPH-Fe complexes on inflammatory response of IDA mice by measuring the levels of TNF-α as well as IL-10 in the colonic tissues of mice, and to explore the modulatory effect of MEPH-Fe complexes on the inflammatory response of IDA mice. TNF-α is the primary pro-inflammatory factor relevant to the pathogenesis of inflammatory bowel disease[44], while IL-10 is an essential anti-inflammatory and immunomodulatory factor[45]. Higher levels of TNF-α in colon

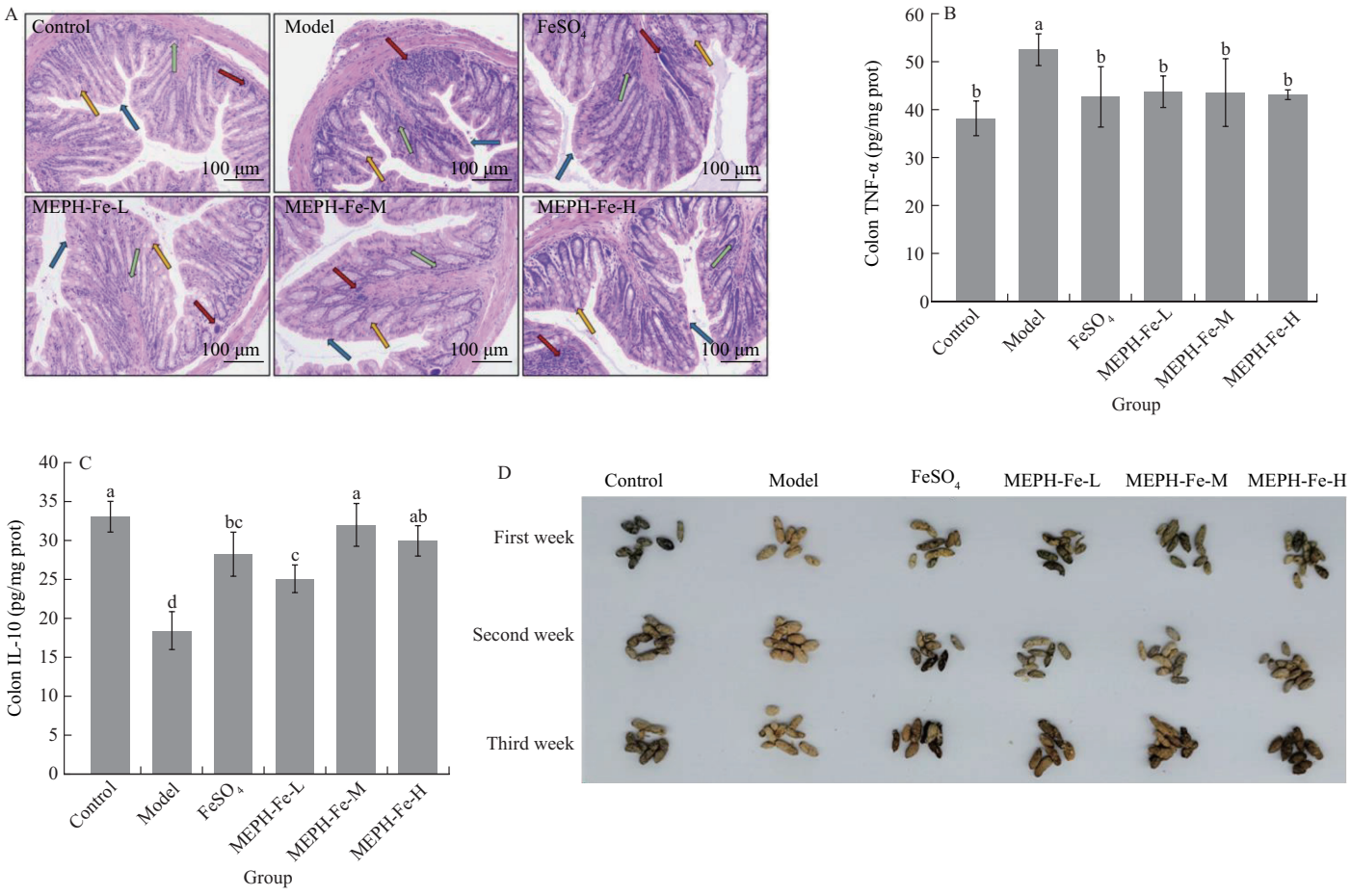

Fig. 6 Effects of MEPH-Fe complexes on the colon tissue and the inflammatory cytokines against IDA. (A) Intestinal histological evaluation by H&E staining, ×200 magnification. Different colored arrows point toward representative tissue counterparts. Red: inflammatory infiltrating cells; green: crypt structure; yellow: goblet cells; and blue: colonic lumen. (B) Value of TNF-α. (C) Value of IL-10. (D) Direct observation of stool color in mice by images. Different letters above the bars indicate significant differences among groups ($P < 0.05$).

tissue indicate a higher level of inflammation, and similarly, higher levels of IL-10 in colon tissue indicate a good inhibition of colonic inflammation. As illustrated in Fig. 6B, the TNF-α content in model group was the highest, while the levels in $FeSO_4$ group and MEPH-Fe groups significantly decreased and returned to normal levels comparable to those in control group. Similarly, the IL-10 content in colonic tissues, depicted in Fig. 6C, showed that model group had significantly lower IL-10 levels than control group ($P < 0.05$). In contrast, the IL-10 content in $FeSO_4$ group and MEPH-Fe groups exhibited notable increases, with a significant difference observed between MEPH-Fe-M group and the $FeSO_4$ group ($P < 0.05$). The secretion of TNF-α is associated with inflammatory responses and tissue cell damage, and several studies have similarly reported significant elevations of TNF-α alongside decreased levels of IL-10 in IDA mice[7,46]. In summary, MEPH-Fe complexes were effective in restoring the biological levels of cytokines in colon tissues to the levels of normal mice, and the medium dose of MEPH-Fe complexes could be the most suitable choices in applications on iron supplementations. Finally, weekly fecal images of mice in each group during gavage of MEPH-Fe complexes and ferrous sulfate were shown in Fig. 6D. During the 3-week gavage period, the feces of the control mice exhibited the dark brown color, indicating normalcy in the absence of any external interference. In contrast, the feces of the model group mice were light yellow, highlighting a significant deviation from the control group. This difference suggested that the iron-deficient diet impacted the mice's physiology. Furthermore, considering the aforementioned indicators, it was plausible that IDA induced intestinal inflammation, which might also result in alterations in the intestinal flora of the mice. Throughout the 3-week gavage period, the feces of mice in both the ferrous sulfate group and the MEPH-Fe group at varying doses exhibited significant changes compared to the model group, gradually returning to dark brown color. This restoration may be attributed to the intervention of additional iron, which appeared to ameliorate the colonic inflammation associated with IDA. Notably, there were no significant differences in the apparent fecal color among ferrous sulfate, MEPH-Fe-L, and MEPH-Fe-M groups. It was noteworthy that the mice in MEPH-Fe-H group exhibited the darkest feces (even darker than the control group), which might indicate the symptomatic manifestation of colitis resulting from excessive iron ion intake (including the massive quantities of unchelated iron ions)[7]. In the future researches, the abundance of MEPH-Fe complexes in the intestinal flora of IDA mice will be further investigated.

4. Conclusion

In summary, MEPH and iron ions could be effectively bound together through carboxyl and amino groups, resulting in the formation of MEPH-Fe complexes that demonstrated enhanced iron-chelating capacity under specific conditions. The binding of iron ions altered the conformational features and microstructure of MEPH, contributing to its excellent stability. Using an IDA mouse model, the MEPH-Fe complexes exhibited favorable restorative effects on hematological indices, antioxidant properties of organs, and colonic inflammation in IDA mice, with effects that surpassed those observed in ferrous sulfate group. Future research will focus on the transport of MEPH-Fe complexes within blood vessels, the mechanisms of accumulation in organs, and the abundance of intestinal flora in IDA mice.

Conflict of interests

The authors declare that they have no known competing financial interests or personal relationships that could have appeared to influence the work reported in this paper.

Acknowledgements

This work was financially supported by National Key R&D Program of China (2023YFD2401502).

Appendix A. Supplementary data

Supplementary data associated with this article can be found, in the online version, at http://doi.org/10.26599/FSHW.2024.9250439.

References

[1] Y. Man, T. Xu, B. Adhikari, et al., Iron supplementation and iron-fortified foods: a review, Crit. Rev. Food Sci. Nutr. 62(16) (2021) 4504-4525. http://dx.doi.org/10.1080/10408398.2021.1876623.

[2] G.J. Anderson, D.M. Frazer, Current understanding of iron homeostasis, Am. J. Clin. Nutr. 106 (2017) 1559S-1566S. http://dx.doi.org/10.3945/ajcn.117.155804.

[3] C. Chen, D.C. Huang, L.Y. Zhao, et al., Preparation and *in vitro* absorption studies of a novel polysaccharide-iron (III) complex from *Flammulina velutipes*, Int. J. Biol. Macromol. 132 (2019) 801-810. http://dx.doi.org/10.1016/j.ijbiomac.2019.04.015.

[4] K. Shubham, T. Anukiruthika, S. Dutta, et al., Iron deficiency anemia: a comprehensive review on iron absorption, bioavailability and emerging food fortification approaches, Trends Food Sci. Tech. 99 (2020) 58-75. http://dx.doi.org/10.1016/j.tifs.2020.02.021.

[5] T. Wang, S. Lin, P. Cui, et al, Antarctic krill derived peptide as a nanocarrier of iron through the gastrointestinal tract, Food Biosci. 36 (2020) 100657. http://dx.doi.org/10.1016/j.fbio.2020.100657.

[6] X. Cheng, L. Guan, M. Muskat, et al., Effects of Ejiao peptide-iron chelates on intestinal inflammation and gut microbiota in iron deficiency anemic mice, Food Funct. 12(21) (2021) 10887-10902. http://dx.doi.org/10.1039/d1fo01802g.

[7] X. Liu, X. Yu, S. Dou, et al., Characterization of oyster protein hydrolysate–iron complexes and their *in vivo* protective effects against iron deficiency-induced symptoms in mice, J. Agric. Food Chem. 71(44) (2023) 16618-16629. http://dx.doi.org/10.1021/acs.jafc.3c05182.

[8] X. Ma, C. Liu, W. Song, et al., Evaluating the efficacy of a ferrous-ion-chelating peptide from Alaska pollock frame for the improvement of iron nutritional status in rats, Food Funct. 10(8) (2019) 4888-4896. http://dx.doi.org/10.1039/c9fo00310j.

[9] B. Li, H. He, W. Shi, et al., Effect of duck egg white peptide-ferrous chelate on iron bioavailability *in vivo* and structure characterization, J. Sci. Food Agric. 99(4) (2018) 1834-1841. http://dx.doi.org/10.1002/jsfa.9377.

[10] Q. Jin, D. Peng, Z. Zheng, Advances in extracting and understanding the bioactivities of marine organism peptides: a review, J. Food Process Pres. 46(6) (2021) 15602. http://dx.doi.org/10.1111/jfpp.15602.

[11] X. Liu, Z. Wang, J. Zhang, et al., Isolation and identification of zinc-chelating peptides from sea cucumber (*Stichopus japonicus*) protein hydrolysate, J. Sci. Food Agric. 99(14) (2019) 6400-6407. http://dx.doi.org/10.1002/jsfa.9919.

[12] Z. Xu, F. Zhao, H. Chen, et al., Nutritional properties and osteogenic activity of enzymatic hydrolysates of proteins from the blue mussel (*Mytilus edulis*), Food Funct. 10(12) (2019) 7745-7754. http://dx.doi.org/10.1039/c9fo01656b.

[13] M. Qiao, M. Tu, H. Chen, et al., Identification and *in silico* prediction of anticoagulant peptides from the enzymatic hydrolysates of *Mytilus edulis* proteins, Int. J. Mol. Sci. 19(7) (2018) 2100. http://dx.doi.org/10.3390/ijms19072100.

[14] T.D.L. Vo, K.T. Pham, V.M.V. Le, et al., Evaluation of iron-binding capacity, amino acid composition, functional properties of *Acetes japonicus* proteolysate and identification of iron-binding peptides, Process Biochem. 91 (2020) 374-386. http://dx.doi.org/10.1016/j.procbio.2020.01.007.

[15] X. Yu, S. Dou, X. Liu, et al, Establishment of oyster protein hydrolysate-chitosan oligosaccharide-zinc delivery system and its characterization, digestion & absorption *in-vitro* and *in-vivo*, Food Biosci. 56 (2023) 103247. http://dx.doi.org/10.1016/j.fbio.2023.103247.

[16] X. Xu, Y. Qiao, B. Shi, et al., Alcalase and bromelain hydrolysis affected physicochemical and functional properties and biological activities of legume proteins, Food Structure 27 (2021) 100178. http://dx.doi.org/10.1016/j.foostr.2021.100178.

[17] H. Zhang, L. Zhao, Q. Shen, et al., Preparation of cattle bone collagen peptides-calcium chelate and its structural characterization and stability, LWT-Food Sci. Technol. 144 (2021) 111264. http://dx.doi.org/10.1016/j.lwt.2021.111264.

[18] W. Huang, Y. Lan, W. Liao, et al., Preparation, characterization and biological activities of egg white peptides-calcium chelate, LWT-Food Sci. Technol. 149 (2021) 112035. http://dx.doi.org/10.1016/j.lwt.2021.112035.

[19] W. Qu, Y. Feng, T. Xiong, et al., Preparation of corn ACE inhibitory peptide-ferrous chelate by dual-frequency ultrasound and its structure and stability analyses, Ultrason. Sonochem. 83 (2022) 105937. https://doi.org/10.1016/j.ultsonch.2022.105937.

[20] X. Wang, A. Gao, Y. Chen, et al., Preparation of cucumber seed peptide-calcium chelate by liquid state fermentation and its characterization, Food Chem. 229 (2017) 487-494. http://dx.doi.org/10.1016/j.foodchem.2017.02.121.

[21] J. Luo, X. Yao, O.P. Soladoye, et al., Phosphorylation modification of collagen peptides from fish bone enhances their calcium-chelating and antioxidant activity, LWT-Food Sci. Technol. 155 (2022) 112978. http://dx.doi.org/10.1016/j.lwt.2021.112978.

[22] W. Wu, L. He, Y. Liang, et al., Preparation process optimization of pig bone collagen peptide-calcium chelate using response surface methodology and its structural characterization and stability analysis, Food Chem. 284 (2019) 80-89. http://dx.doi.org/10.1016/j.foodchem.2019.01.103.

[23] S. Lin, X. Hu, L. Li, et al., Preparation, purification and identification of iron-chelating peptides derived from tilapia (*Oreochromis niloticus*) skin collagen and characterization of the peptide-iron complexes, LWT-Food Sci. Technol. 149 (2021) 111796. http://dx.doi.org/10.1016/j.lwt.2021.111796.

[24] N. Sun, Y. Wang, Z. Bao, et al., Calcium binding to herring egg phosphopeptides: binding characteristics, conformational structure and intermolecular forces, Food Chem. 310 (2020) 125867. http://dx.doi.org/10.1016/j.foodchem.2019.125867.

[25] L. Wang, Y. Ding, X. Zhang, et al., Isolation of a novel calcium-binding peptide from wheat germ protein hydrolysates and the prediction for its mechanism of combination, Food Chem. 239 (2018) 416-426. http://dx.doi.org/10.1016/j.foodchem.2017.06.090.

[26] W. Wu, J. Jia, C. Wen, et al., Optimization of ultrasound assisted extraction of abalone viscera protein and its effect on the iron-chelating activity, Ultrason. Sonochem. 77 (2021) 105670. http://dx.doi.org/10.1016/j.ultsonch.2021.105670.

[27] X. Wu, F. Wang, X. Cai, et al., Glycosylated peptide-calcium chelate: characterization, calcium absorption promotion and prebiotic effect, Food Chem. 403 (2023) 134335. http://dx.doi.org/10.1016/j.foodchem.2022.134335

[28] R. Sun, X. Liu, Y. Yu, et al., Preparation process optimization, structural characterization and *in vitro* digestion stability analysis of Antarctic krill (*Euphausia superba*) peptides-zinc chelate, Food Chem. 340 (2021) 128056. http://dx.doi.org/10.1016/j.foodchem.2020.128056.

[29] C. Wang, B. Li, B. Wang, et al., Degradation and antioxidant activities of peptides and zinc–peptide complexes during *in vitro* gastrointestinal digestion, Food Chem. 173 (2015) 733-740. http://dx.doi.org/10.1016/j.foodchem.2014.10.066.

[30] Z. Zhang, F. Zhou, X. Liu, et al., Particulate nanocomposite from oyster (*Crassostrea rivularis*) hydrolysates *via* zinc chelation improves zinc solubility and peptide activity, Food Chem. 258 (2018) 269-277. http://dx.doi.org/10.1016/j.foodchem.2018.03.030.

[31] P. Cui, S. Lin, Z. Jin, et al., *In vitro* digestion profile and calcium absorption studies of a sea cucumber ovum derived heptapeptide–calcium complex, Food Funct. 9(9) (2018) 4582-4592. http://dx.doi.org/10.1039/c8fo00910d.

[32] J. Zhang, L. Liang, Z. Tian, et al., Preparation and *in vitro* evaluation of calcium-induced soy protein isolate nanoparticles and their formation mechanism study, Food Chem. 133(2) (2012) 390-399. http://dx.doi.org/10.1016/j.foodchem.2012.01.049.

[33] J. Lin, X. Cai, M. Tang, et al., Preparation and evaluation of the chelating nanocomposite fabricated with marine algae *Schizochytrium* sp. protein hydrolysate and calcium, J. Agric. Food Chem. 63(44) (2015) 9704-9714. http://dx.doi.org/10.1021/acs.jafc.5b04001.

[34] L. Qi, H. Zhang, Y. Guo, et al., A novel calcium-binding peptide from bovine bone collagen hydrolysate and chelation mechanism and calcium absorption activity of peptide-calcium chelate, Food Chem. 410 (2023) 135387. http://dx.doi.org/10.1016/j.foodchem.2023.135387.

[35] Y. He, P. Yang, Y. Ding, et al., The preparation, antioxidant activity evaluation, and iron-deficient anemic improvement of oat (*Avena sativa* L.) peptides–ferrous chelate, Front. Nutr. 8 (2021) 687133. http://dx.doi.org/10.3389/fnut.2021.687133.

[36] X. Cheng, Y. Chen, C. Cao, et al., Ejiao peptide-iron chelates regulate the metabolism of iron deficiency anemia mice and improve the bioavailability of iron, Food Bio. 54 (2023) 102835. http://dx.doi.org/10.1016/j.fbio.2023.102835.

[37] S. Lewis, A. Williams, S. Eisenbarth, Structure and function of the immune system in the spleen, Sci. Immunol. 4(33) (2019). http://dx.doi.org/10.1126/sciimmunol.aau6085.

[38] S. Hu, S. Lin, Q. Feng, et al., Iron complexes with antarctic krill–derived peptides show superior effectiveness to their original protein–iron complexes in mice with iron deficiency anemia, Nutrients 15(11) (2023). http://dx.doi.org/10.3390/nu15112510

[39] M. Chen, C. Chen, Y. Zhang, et al., Effects of iron-peptides chelate nanoliposomes on iron supplementation in rats, Biol. Trace Elem. Res. 201(9) (2022) 4508-4517. http://dx.doi.org/10.1007/s12011-022-03539-2.

[40] S. Song, L. Yang, M. Ye, et al., Antioxidant activity of a *Lachnum* YM226 melanin–iron complex and its influence on cytokine production in mice with iron deficiency anemia, Food Funct. 7(3) (2016) 1508-1514. http://dx.doi.org/10.1039/c5fo01274k.

[41] N. Jia, H. Qiao, W. Zhu, et al., Antioxidant, immunomodulatory, oxidative stress inhibitory and iron supplementation effect of *Astragalus membranaceus* polysaccharide-iron (III) complex on iron-deficiency anemia mouse model, Int. J. Biol. Macromol. 132 (2019) 213-221. http://dx.doi.org/10.1016/j.ijbiomac.2019.03.196.

[42] N. Tang, L. Chen, H. Zhuang, Effects of heme iron enriched peptide on iron deficiency anemia in rats, Food Funct. 5(2) (2014) 390-399. http://dx.doi.org/10.1039/c3fo60292c.

[43] C. Huo, G. Li, Y. Hu, et al., The impacts of iron overload and ferroptosis on intestinal mucosal homeostasis and inflammation, Int. J. Mol. Sci. 23(22) (2022) 14195. http://dx.doi.org/10.3390/ijms232214195.

[44] M. Friedrich, M. Pohin, F. Powrie, Cytokine networks in the pathophysiology of inflammatory bowel disease, Immunity 50(4) (2019) 992-1006. http://dx.doi.org/10.1016/j.immuni.2019.03.017.

[45] A. Rajasekaran, V. Shivakumar, S.V. Kalmady, et al., The impact of IL10 polymorphisms and sHLA-G levels on the risk of schizophrenia, Asian J. Psychiatr. 23 (2016) 39-43. http://dx.doi.org/10.1016/j.ajp.2016.06.018.

[46] J. Zhou, X. Mao, X. Wang, et al., Anti-anaemia efficacy of *β*-lactoglobulin hydrolysate-iron complex on iron-deficient anaemic rats, Eur. J. Nutr. 53(3) (2013) 877-884. http://dx.doi.org/10.1007/s00394-013-0591-x.